Title
Synthesis of Nickel(I)-Bromide Complexes via Oxidation and Ligand Displacement: Evaluation of Ligand Effects on Speciation and Reactivity.

Journal
Journal of the American Chemical Society, 145(35)

Authors
Newman-Stonebraker, Samuel
Raab, T
Roshandel, Hootan
et al.

Publication Date
2023-09-06

DOI
10.1021/jacs.3c06233

Peer reviewed

HHS Public Access

Author manuscript

J Am Chem Soc. Author manuscript; available in PMC 2023 October 31.

Published in final edited form as:

J Am Chem Soc. 2023 September 06; 145(35): 19368–19377. doi:10.1021/jacs.3c06233.

Synthesis of Nickel(I)–Bromide Complexes via Oxidation and Ligand Displacement: Evaluation of Ligand Effects on Speciation and Reactivity

Samuel H. Newman-Stonebraker[a,b,‡], **T. Judah Raab**[b,‡], **Hootan Roshandel**[b], **Abigail G. Doyle**[b]

[a]Department of Chemistry, Princeton University, Princeton, New Jersey 08544, USA

[b]Department of Chemistry and Biochemistry, University of California Los Angeles, Los Angeles, California 90095, USA

Abstract

Nickel's +1 oxidation state has received much interest due to its varied and often enigmatic behavior in increasingly popular catalytic methods. In part, the lack of understanding about Ni^{I} results from common synthetic strategies limiting the breadth of complexes that are accessible for mechanistic study and catalyst design. We report an oxidative approach using tribromide salts that allows for the generation of a well-defined precursor, $[Ni^{I}(COD)Br]_2$, as well as several new Ni^{I} complexes. Included among them are complexes bearing bulky monophosphines, for which structure–speciation relationships are established and catalytic reactivity in a Suzuki-Miyaura coupling (SMC) is investigated. Notably, these routes also allow for the synthesis of well-defined monomeric $^{t\text{-}Bu}$bpy-bound Ni^{I} complexes, which has not previously been achieved. These complexes, which react with aryl halides, can enable previously challenging mechanistic investigations and present new opportunities for catalysis and synthesis.

Graphical Abstract

Corresponding Author: **Abigail G. Doyle** – Department of Chemistry and Biochemistry, University of California Los Angeles, Los Angeles, California 90095, United States; agdoyle@chem.ucla.edu.

†**Present Addresses**: Department of Chemistry, Yale University, New Haven, CT 06511, United States.

Samuel H. Newman-Stonebraker† – Department of Chemistry, Princeton University, Princeton, New Jersey 08544, United States; Department of Chemistry and Biochemistry, University of California Los Angeles, Los Angeles, California 90095, United States;

T. Judah Raab – Department of Chemistry and Biochemistry, University of California Los Angeles, Los Angeles, California 90095, United States;

Hootan Roshandel – Department of Chemistry and Biochemistry, University of California Los Angeles, Los Angeles, California 90095, United States;

‡S. H. N.-S. and T. J. R. contributed equally and are listed in alphabetical order.

The authors declare no competing financial interest.

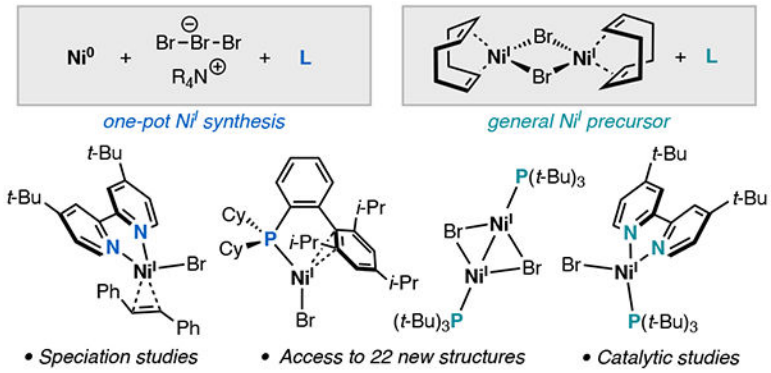

INTRODUCTION

Nickel-catalyzed cross-couplings have emerged as broadly useful methodologies in synthetic organic chemistry—in large part due to the complementary reactivity of Ni to precious metals like Pd.[1,2] In addition to Ni's ability to facilitate challenging oxidative addition reactions,[3,4] its relative propensity[5] to access open-shell electron configurations (i.e., Ni^{I} & Ni^{III}) underlies many modern cross-coupling reactions (e.g., Ni/photoredox,[6] Ni/electrocatalysis,[7] crosselectrophile coupling[8]). Organometallic Ni^{I} species are also important intermediates for catalytic CO_2 insertion reactions.[9–12] Conversely, open-shell intermediates can attenuate turnover in traditional Ni^{0}/Ni^{II} cycles, where Ni^{I} species have been identified as off-cycle.[13] It is therefore of great interest to understand the nuanced factors that control the formation, reactivity, and speciation of Ni^{I} intermediates.[14,15]

Stoichiometric synthesis of well-defined Ni^{I} complexes presents an opportunity to investigate these nuances and characterize species that are relevant in catalysis. Examples of such investigations have examined several ligand classes on Ni^{I} centers: Matsubara[16] and Schoenebeck[17] have studied *N*-heterocyclic carbene (NHC) ligands, Hazari[13,18–20] and Schoenebeck[21] bisphosphine ligands, and Hazari[9,22] and Martin[9,23] phenanthroline ligands. For each ligand class, tractable conclusions about the role(s) of Ni^{I} species in the respective catalytic mechanisms have been put forth. However, existing strategies for synthesizing Ni^{I} species (Figure 1A) limit the breadth of complexes that can be accessed with catalytically relevant ligands. We postulate two contributing factors therein: (1) common preparations for Ni^{I} species typically necessitate the formation of $L_nNi^{II}X_2$ complexes that are intractable for bulky ligands[24] and (2) components of [Ni^{0}] and [Ni^{II}] precursors used for Ni^{I} synthesis can induce undesired redox equilibria and speciation effects.[23,25] These limitations are borne out in a literature survey of Ni^{I} complexes: certain structural motifs are well-explored while others remain elusive (Figure 1B).

Bulky monophosphines are among the ligand classes that have scarcely been characterized on Ni^{I} centers. Notably, small monophosphine ligands have been known to form monomeric $(PR_3)_nNi^{I}X$ (n = 2 or 3) species via comproportionation and oxidative addition,[26,27] but dimeric $[(PR_3)Ni^{I}X]_2$ complexes bearing larger phosphine congeners were unknown prior to a 2022 publication from our group and Schoenebeck's report concurrent to this work.[28,29] This is in stark contrast to precedent for PdI, for which complexes of the type $[(PR_3)Pd^{I}X]_2$

are long-known[30] and have been thoroughly studied by Schoenebeck and coworkers.[31,32] As precedent for bisligated $(PR_3)_2Ni^I$ species has shown that such species are capable of catalytic cycle (re)entry,[13,18–20] the structure and speciation of monoligated $(PR_3)Ni^I$ complexes warrants further investigation.

Moreover, while 4,4'-di-*tert*-butylbipyridine ($^{t\text{-Bu}}$bpy) is the ligand of choice for many Ni-catalyzed cross-couplings that invoke open-shell intermediates,[33–36] only two examples of formal ($^{t\text{-Bu}}$bpy)Ni^I species have been structurally characterized: Hazari's [($^{t\text{-Bu}}$bpy)Ni^ICl]$_2$ and Nocera's [($^{t\text{-Bu}}$bpy)$Ni^{1.5+}$(quinuclidine)Cl]$_2$Cl.[22,37] Importantly, these complexes do not replicate the behavior of ($^{t\text{-Bu}}$bpy)Ni^I species in catalysis due to irreversible dimerization of reactive ($^{t\text{-Bu}}$bpy)Ni^IX. While *in situ* generation of monomeric ($^{t\text{-Bu}}$bpy)Ni^I species has clarified the reactivity of important catalytic intermediates,[38,39] these approaches are more challenging to apply to future catalyst design and mechanistic studies than stoichiometric synthesis.

Strategies to enable the synthesis of previously unknown Ni^I complexes create downstream opportunities for more effective Ni catalysis. Contributions from Morandi and coworkers, who recently reported a phenoxide-bound Ni^I precursor,[40] have already led to mechanistic insight and development in Ni-catalyzed methodologies.[41] Further goals for the synthetic organometallic community in this area include: the complexation of catalytically relevant ligands to structurally novel Ni^I centers, the incorporation of easily derivatized X-type ligands such as halides, and application of synthetic discoveries to catalytic systems.

Herein, we present the synthesis of over 20 previously unidentified Ni^I complexes bearing olefins and catalytically relevant monophosphines and bipyridine ligands. We access these complexes through a mild one-pot oxidation or via ligand displacement of well-defined Ni^I precursors. For the bulky monophosphine class, we conduct a structure–speciation analysis and catalytic studies to elucidate these ligands' behavior on Ni^I centers. For the bipyridine class, we identify the first examples of monomeric ($^{t\text{-Bu}}$bpy)Ni^I complexes and investigate their electronic structure and stoichiometric reactivity with aryl halides.

RESULTS AND DISCUSSION

In our recent study of dialklylbiaryl phosphine ligands in Ni catalysis, we serendipitously identified the structure of a unique monophosphine-bound Ni^I halide dimer.[28] This species, [(CyJohnPhos)Ni^ICl]$_2$ (**1-Cl**), formed in trace amounts following oxidative addition of 2-chlorotoluene to (CyJohnPhos)$_2Ni^0$. To the best of our knowledge, **1-Cl** was the first structurally characterized example of a [$(PR_3)Ni^IX]_2$ dimer. To further investigate the role of **1** in the catalytic system of interest, we sought to synthesize this complex independently by comproportionation. However, comproportionation attempts with several Ni^0 and Ni^{II} precursors failed, perhaps due to challenges forming ligated $Ni^{II}Cl_2$ species with CyJohnPhos. Taking inspiration from studies from Fout[42] and Uyeda[43], we were able to isolate [(CyJohnPhos)Ni^IBr]$_2$ (**1-Br**) by oxidizing (CyJohnPhos)$_2Ni^0$ with trimethylphenylammonium tribromide (TMPhATB), a commercially available, easily manipulated solid (Figure 2B). **1-Br** assumes an analogous solid-state structure to **1-Cl**, with

κ^1-P phosphine binding, μ_2-Br ligand bridging, and a Ni–Ni bonding interaction (2.5955(4) Å).

Seeking to extend this oxidative approach to bulkier Buchwald phosphines, we treated $Ni(COD)_2$ (COD = 1,5-cyclooctadiene) with TMPhATB in the presence of XPhos, generating (XPhos)Ni^IBr (**2**). In the solid state, **2** is monomeric, with XPhos adopting a κ^1-P, η^2-C_{arene} binding mode. This speciation contrasts with both **1-Cl** and **1-Br**, in which CyJohnPhos binds κ^1-P only in a dimeric complex. EPR measurements in glassy toluene at 77 K suggest that the solid-state speciation is conserved in the solution phase: no signal is observed for **1-Br**, while spectra of **2** feature a rhombic signal with large hyperfine splitting from the ^{31}P nucleus of XPhos (Figure 2D). The low solubility of **1-Br** in organic solvents prevented the measurement of its solution magnetic moment. However, **2** was observed to have a solution-phase magnetic moment of 1.73 μ_B, consistent with a monomeric d^9 species.[44]

Having identified tribromide oxidation as a tenable route to Ni^I species, we sought to evaluate the scope of ligands that could be complexed to Ni^I centers. We were able to generate Ni^I halide complexes for a variety of catalytically important ligand classes including mono- and bisphosphine, *N*-heterocyclic carbene (NHC), and polypyridyl (Table 1). In most cases, yields are comparable to other reported syntheses,[4,17,45–47] but the unique generality of Br_3^- oxidation is highly enabling.

However, challenges arose in the isolation of Ni^I complexes bearing two ligand classes: bipyridines and bulky trialkylphosphines. The former case will be discussed in detail (*vide infra*). Our challenges with the latter case are best summarized with the product mixture resulting from the oxidation of a $Ni(COD)_2$/P(*t*-Bu)$_3$ mixture. The desired product, the dimeric [(P(*t*-Bu)$_3$)Ni^IBr]$_2$ complex, was not detected. Instead, this reaction generated two unanticipated P(*t*-Bu)$_3$-bound species: an over-oxidized $Ni^{1.5+}$ dimer, [(P(*t*-Bu)$_3$)$_2$$Ni^{1.5+}{}_2Br_3$] (**3**), and a nickelate complex with an outersphere ammonium cation, [Me_3PhN][(P(*t*-Bu)$_3$)Ni^IBr$_2$] (**4**) (Figure 3). Complex **3** likely forms as a product along with Ni^0 black in a redox equilibrium with the expected Ni^I dimer, while **4** is presumably the product of trimethylphenylammonium coordination to a (P(*t*-Bu)$_3$)Ni^IBr species.

While complexes **3** and **4** are interesting from a structural and electronic perspective, we sought an alternative route to the desired [(P(*t*-Bu)$_3$)Ni^IBr]$_2$ complex that did not employ ammonium salts. To this end, we identified that the formation of complexes **2**, **3**, and **4** implies a reactive intermediate from which ligation of these bulky phosphines is relatively facile. Both XPhos and P(*t*-Bu)$_3$ are too sterically encumbered to displace COD from $Ni(COD)_2$ directly,[28] but both ligate to Ni following tribromide oxidation. We therefore aimed to isolate this putative intermediate, which could serve as an ammonium-free Ni^I precursor.

Following tribromide oxidation of a $Ni(COD)_2$ solution in THF-d_8, we observed the formation of a single paramagnetic species by ^{1}H NMR. Use of a more soluble tribromide oxidant, tetrabutylammonium tribromide (TBATB),[48] cooling, and addition of solvent quantities of free COD to the oxidation mixture stabilized the resulting complex. With these

modifications, we were able to isolate and characterize $[Ni^{I}(COD)Br]_2$ (**5**), a golden yellow solid that is stable at −35 °C under inert atmosphere (Figure 4).[49,50] **5** is a rare example of a Ni^{I}–olefin complex and a tractable precursor to a variety of Ni^{I}–Br complexes (*vide infra*).

Structure–Speciation Relationships of Monodentate Phosphines with $[Ni^{I}(COD)Br]_2$.

With access to $[Ni^{I}(COD)Br]_2$, we studied its ability to serve as a precursor to generate L_nNi^{I} complexes with bulky monophosphines. Unlike with $Ni(COD)_2$,[28] Buchwald-type ligands of all steric profiles were capable of displacing the COD ligands of $[Ni^{I}(COD)Br]_2$ to generate the desired Ni^{I} complex. In addition to **1-Br** and **2** with CyJohnPhos and XPhos, respectively, Ni^{I} complexes with SPhos, DavePhos, JohnPhos, and *t*-BuBrettPhos formed readily from **5**; each of these complexes was characterized by SCXRD (see SI). For Buchwald-type ligands, three distinct classes of L_1Ni^{I} species were observed in the solid state (Figure 5): (i) dimers with Ni–Ni bonds and no η^2-C_{arene} interaction (e.g., **1-Br**), (ii) dimers with no Ni–Ni bond (distances >3.0 Å) and a strong η^2-C_{arene} interaction between each Ni and the ligand B ring (e.g., $[(JohnPhos)Ni^{I}Br]_2$, **6**), and (iii) monomers with a strong η^2-C_{arene} interaction to the B ring (e.g., **2**). The ligand structural feature that most clearly leads to the observed speciation outcome is the presence of a 4-*i*-Pr group on the B ring, which prevents dimer formation altogether. The structural feature(s) that distinguishes the two classes of dimers is less clear, though only the smaller Buchwald-type ligands formed species with Ni–Ni bonds. Furthermore, the dimeric complexes **1-Br** and **6** are believed to exhibit fluxional behavior between binding modes in solution (see SI).

Given the success of bulky Buchwald-type ligands at displacing COD from **5**, we reexamined the synthesis of bulky trialkylphosphine-bound Ni^{I} complexes using **5** as a precursor (Figure 6). We were pleased to find that reaction of **5** with 2 equiv of P(*t*-Bu)$_3$ (1:1 L:Ni) led to the formation of $[(P(t\text{-}Bu)_3)Ni^{I}Br]_2$ (**7**). The X-ray crystal structure of **7** confirmed its identity as a Ni^{I} dimer, with a Ni–Ni bond distance (2.6005(6) Å) similar to that observed in **1-Br**. We found that P(*t*-Bu)$_3$:Ni ratios >1:1 did not affect the speciation of the resulting complexes, with only the L_1Ni^{I} dimer complex observed.

Recent work by our lab and the Sigman lab has found that minimum percent buried volume (% V_{bur} (*min*))—a steric quantification of the smallest energetically accessible conformation of a ligand within 3.5 Å of the metal center—enables the discovery of structure–speciation relationships of phosphine ligand/metal complexes in cross-coupling.[51] With the demonstrated success of % V_{bur} (*min*) in rationalizing phosphine ligand effects at Ni^0/Ni^{II}, we were curious to investigate similar effects at Ni^{I}.

For ligands with % V_{bur} (*min*) values[52] slightly lower than P(*t*-Bu)$_3$ (36.3%), such as CyP(*t*-Bu)$_2$ (34.3%) and Cy$_2$P(*t*-Bu) (32.0%), both the L_1Ni dimer[53](**8** (L = CyP(*t*-Bu)$_2$) and **9** (L = Cy$_2$P(*t*-Bu))) and L_2Ni^{I} monomer species (**10** (L = CyP(*t*-Bu)$_2$) and **11** (L = Cy$_2$P(*t*-Bu))) could be generated and structurally characterized, with the L:Ni stoichiometric ratio controlling the outcome.[54] While these ligands normally do not form L_2Ni complexes at Ni^0 or Ni^{II}, the relatively small size of the single halide ligand leaves the majority of Ni's coordination sphere unencumbered, allowing the coordination of large phosphines. The crystal structure of $[(CyP(t\text{-}Bu)_2)_2Ni^{I}Br]$ revealed a nearly T-shaped complex, as the high

amount of steric pressure between the bulky phosphines distorted the complex from the ideal trigonal geometry. For ligands smaller than P(*t*-Bu)$_3$ where more than one Ni^I species can form, L:Ni stoichiometry controlled the outcome for isolated material in the solid state. These trends were generally conserved in solution-state NMR characterization, though a small amount of phosphine dissociation and dimerization was observed for L$_2$Ni^I monomer **10** with CyP(*t*-Bu)$_2$ (see SI).

We also found that PCy$_3$ (% V_{bur} (*min*) = 30.2 %) could form a L$_1$Ni^I dimer (**12** (L = PCy$_3$)) from **5** with a 1:1 ratio of phosphine:Ni. In the presence of excess COD, the PCy$_3$ complex is more prone to disproportionation—generating Ni(COD)$_2$ and (PCy$_3$)$_2$Ni^{II}Br$_2$—than ligands with higher %V$_{bur}$ (*min*) values. This is unsurprising given that stable L$_2$Ni^0 and L$_2$Ni^{II} complexes can readily form with PCy$_3$.[24,51,55,56] Nonetheless, the ability to synthesize [(PCy$_3$)Ni^{I}Br]$_2$ differs from the ligand structure–speciation trends observed in generation of the analogous PdI dimers.[32] Like CyP(*t*-Bu)$_2$ and Cy$_2$P(*t*-Bu), the L$_2$Ni^{I}Br monomer (**13** (L = PCy$_3$)) was readily obtained with PCy$_3$.

For even smaller PPh$_3$ (% V_{bur} (*min*) = 28.2 %), Ni^I species were obtainable for 3:1, 2:1, and 1:1 ratios of phosphine:Ni. Unlike the examined phosphines with greater %V$_{bur}$ (*min*) values, a L$_3$Ni^I (**14** (L = PPh$_3$)) monomer is sterically accessible for PPh$_3$. The L$_2$Ni^I (**15** (L = PPh$_3$)) monomer is also isolable. Uniquely, treatment of **5** with only one equivalent of PPh$_3$ relative to Ni resulted in the formation of a rare monomeric COD-bound Ni^I complex, (PPh$_3$)Ni^I(COD)Br (**16**) (Figure 6B).[57] Similar to COD-bound **5**, complex **16** rapidly decomposes in solution in the absence of added COD or ligand.

Overall, we have found that [Ni^I(COD)Br]$_2$ is a versatile precursor for synthesizing monophosphine-bound Ni^I complexes. The ease of COD displacement from **5** enables formation of otherwise challenging-to-access complexes with bulky phosphines such as Buchwald-type ligands and P(*t*-Bu)$_3$. Furthermore, the excellent stoichiometric control on product outcome when using **5** as a precursor allows for a detailed understanding of phosphine structural effects on Ni^I speciation (Figure 6).

Implications of Bulky Monophosphine Speciation at Ni^I in Cross-Coupling.

Recently, in a collaborative study with the Sigman group, we identified phosphine ligand reactivity thresholds in Ni- and Pd-catalyzed cross-coupling datasets;[51] these reactivity thresholds were linked to the % V_{bur} (*min*) steric descriptor.[52] For Ni, only monodentate phosphines with % V_{bur} (*min*) values less than 32% (e.g., CyTyrannoPhos, PPh$_3$, and PCy$_3$) were effective at catalyzing the studied Suzuki–Miyaura coupling (SMC) reactions. This value corresponded to the region of chemical space where two phosphines could bind and stabilize Ni^0 and Ni^{II} complexes; these even oxidation states of Ni are believed to be the catalytically relevant species in SMC reactions.[13] Given Ni's propensity to engage in unproductive side pathways, we hypothesized that attaining bisligated Ni^0/Ni^{II} complexes was necessary to stabilize these on-cycle species.[58] The inability of bulky monodentate phosphines (i.e., with % V_{bur} (*min*) values greater than 32%) to adequately stabilize these species would leave Ni more prone to falling into off-cycle thermodynamic sinks. However, this hypothesis has eluded testing due to previous synthetic challenges in accessing Ni complexes of any oxidation state with bulky monodentate phosphines. Indeed, ligands like

P(*t*-Bu)$_3$ do not displace olefin ligands from Ni^0 precursors like Ni(COD)$_2$,[28] nor do they ligate Ni^{II}X$_2$ salts.[24]

Given the demonstrated ability of well-defined, bidentate phosphine-bound Ni^I complexes to re-enter Ni^0/Ni^{II} catalytic cycles,[19] we were interested to determine if monodentate phosphine-bound Ni^I complexes could also reenter the cycle and if the % V_{bur} (*min*) threshold behavior was retained. In order to evaluate the behavior of these monophosphine Ni^I species in a catalytic system, [Ni^I(COD)Br]$_2$ was employed as a precatalyst in two SMC reactions (Figure 7A). For the three phosphines tested with % V_{bur} (*min*) values less than 32%, the observed yields are lower when [Ni^I(COD)Br]$_2$ is used as a precursor relative to Ni(COD)$_2$, in line with previous precedent with dppf/Ni^I species. However, moderate product formation did occur for these three ligands, indicating entry to the Ni$^{0/II}$ cycle. A notable decline in yield occurs for monophosphines possessing % V_{bur} (min) values >32%, analogous to the reactivity threshold we recently reported with Ni(COD)$_2$ as a precursor. Even in the absence of COD, isolated P(*t*-Bu)$_3$ dimer **7** was an ineffective precatalyst, giving trace yields in both reactions.

These data suggest that Ni^I complexes bound by monophosphines with % V_{bur} (*min*) values > 32% are more recalcitrant towards Ni$^{0/II}$ SMC catalytic cycle reentry than those bound by monophosphines with % V_{bur} (*min*) values < 32%. The ability to coordinate two or more phosphine ligands to substrate bound Ni^0 or Ni^{II} complexes appears to be necessary for stability of these even oxidation state species in catalysis. The unique geometric and electronic structure of Ni^I monomer and dimer species appears to be ideal for supporting bulky ligands, whereas typical coordination spheres of Ni^0 and/or Ni^{II} complexes are not amenable to coordination of multiple bulky phosphines (Figure 7B). This prevents monophosphines with % V_{bur} (*min*) values > 32% from being effective in the SMC reactions studied, even if ligated, well-defined Ni species like **7** are utilized.

Synthesis of Ni^I Complexes with Bipyridine Ligands.

Motivated by the catalytic importance of $^{t\text{-Bu}}$bpy, we sought to access ($^{t\text{-Bu}}$bpy)Ni^I complexes using the synthetic methods discussed thus far. Tribromide oxidation of a Ni(COD)$_2$/$^{t\text{-Bu}}$bpy mixture did not afford isolable Ni^I species; bidentate, **π**-accepting COD induced the formation of COD-bound Ni^0 and L$_n$NiBr$_2$ species upon concentration (Table 1).[25] Like-wise, reaction of $^{t\text{-Bu}}$bpy with the well-defined precursor **5** did not afford isolable [($^{t\text{-Bu}}$bpy)Ni^{I}Br]$_2$. With these results in hand, we envisioned that reaction of $^{t\text{-Bu}}$bpy with precursors that contain supporting ligands other than COD would enable access to Ni^I complexes of catalytic interest.

First, we investigated bulky monophosphine-bound Ni^I dimers as synthetic precursors of ($^{t\text{-Bu}}$bpy)Ni^I complexes. Matsubara and coworkers have previously demonstrated that unsubstituted 2,2'-bipyridine (bpy) could displace the bridging μ-Cl/Br interactions of NHC-bound Ni^I halide dimers to give monomeric (NHC)(bpy)Ni^{I}X complexes.16 We evaluated an analogous route from **7** and were able to isolate (*t*-Bubpy)(P*t*-Bu3)Ni^{I}Br (**17**) by facile ligand displacement. By varying bipyridine ligand identity, it was also possible to identify (CO2Etbpy)(P(*t*-Bu)3)Ni^{I}Br (see SI, CO2Etbpy = diethyl 2,2'-bipyridine-4,4'-dicarboxylate). Indeed, the affinity of large phosphines for the steric environment of Ni^I

species (*vide supra*) seems to favor the formation of monomeric species in heteroleptic complexes with bipyridine ligands. It is exciting to recognize the synergy of this relationship: monomeric bipyridine-ligated Ni^{I} systems are coveted. Furthermore, this class of compounds may suggest previously unexplored mechanistic possibilities for methodologies in which both (poly)pyridyl and bulky monophosphine ligands are employed in one pot.[59,60]

However, we foresaw potential limitations of a (t-^{Bu}bpy)Ni^{I} complex bearing a strongly **σ**-donating phosphine ligand. Such a mixed-ligand system may lead to ambiguity about which ancillary ligand is responsible for reactivity, among other shortcomings. A more general monomeric (t-^{Bu}bpy)(L)Ni^{I}X precursor would fill its coordination sphere with a highly labile ligand, such as an olefin. To this end, we attempted a tribromide oxidation from a different olefin-bound Ni^{0} precursor, $Ni^{0}(stb)_3$ (stb = (*E*)-stilbene).[61,62] Upon treatment of a $Ni^{0}(stb)_3$/t-^{Bu}bpy mixture with 0.5 equiv TBATB, we observed the formation of a previously undetected paramagnetic species by ^{1}H NMR. Layering the resulting THF solution with pentane and cooling to −35 °C afforded red-black crystals suitable for SCXRD, which identified the complex (t-^{Bu}bpy)Ni^{I}(stb)Br (**18**).

Solid-state structural analysis of **17** and **18** reveals subtle differences in the coordination sphere of the metal center (Figure 8D). The t-^{Bu}bpy ligand of **17** is positioned closer to Ni than in **18**, while **18** features a more tightly bound bromo ligand. The Ni–P(t-Bu)$_3$ bond of **17** is longer than for bpy–free congeners **4** and **10**, consistent with greater steric hindrance around the metal center. Bond metrics on the t-^{Bu}bpy ligand are within error for the two complexes, suggesting a similar extent of donation from the Ni^{I} center. The C_2–$C_{2'}$ bonds in the backbones of the t-^{Bu}bpy ligands for **17** and **18** are significantly longer than in (t-^{Bu}bpy)$_2Ni^{0}$ (C_2–$C_{2'}$ = 1.439(6) Å, see SI). This observation is consistent with a relatively **π**-basic metal center endowing greater t-^{Bu}bpy$^{\bullet-}$ character for Ni^{0} species.[43] Also in accordance with **π**-basicity, **18** is observed to activate the olefin of stilbene to a lesser extent than its Ni^{0} congener, (t-^{Bu}bpy)Ni^{0}(stb) (**19**).

The electronic structure of these complexes was studied with EPR spectroscopy (Figure 8E). Continuous-wave spectra of **17** and **18** in glassy frozen solutions afforded rhombic signals. The spectrum of a frozen toluene solution containing **17** features no resolved hyperfine splitting and an observed value of g_{avg} = 2.261, which is similar to previous reports of well-defined monomeric (bpy/phen)Ni^{I}(halide) complexes (g_{avg} = 2.19–2.24).[19,25,63,64] For **18**, a color change from dark green to red was observed upon freezing in both 2-MeTHF and toluene, and spectra exhibited abnormal line-shape (see SI). Thorough investigation of a chemical process that may be occur ring upon freezing has not been conducted, as spin relaxation for **18** is sufficiently long to observe a room-temperature spectrum. The observed g_{iso} value is 2.211, which is also consistent with prior reports.[19,25,63,64] Overall, both EPR spectra are consistent with monomeric d^9 Ni^{I} complexes as observed by SCXRD.

Complexes **17** and **18** are the first structurally characterized monomeric t-^{Bu}bpy-bound Ni^{I} complexes. The nuclearity of similar complexes is observed to be crucial to their reactivity: dimeric [(t-^{Bu}bpy)Ni^{I}X]$_2$ species (X = Cl, Br) cannot kinetically disaggregate and therefore are inert towards aryl halides (Figure 8A),[22] whereas *in situ* generated monomeric

(t-^{Bu}bpy)Ni^{I}X species have been shown to activate even aryl chlorides.[39] Indeed, **17** and **18** are capable of activating aryl halide bonds (Figure 8B). Furthermore, complex **18** is an especially useful Ni^{I} model system for mechanistic and stoichiometric studies: it has a direct Ni^{0} analog, **19**, against which its reactivity can be evaluated. A three-step, two-pot synthesis from Ni(acac)$_2$—which proceeds via **19**—ultimately provided **18** cleanly (Figure 8C). Efforts to prepare **17** through an analogous pathway were unsuccessful, likely due to the instability of a putatively trigonal planar (t-^{Bu}bpy)(P(t-Bu)$_3$)Ni^{0} complex.

Interested in evaluating the reactivity of these monomeric (t-^{Bu}bpy)(L)Ni^{I}Br complexes, we undertook stoichiometric oxidative addition experiments (Figure 9). Both **17** and **18** are observed to react with 1,4-bromofluorobenzene, affording a mixture of (t-^{Bu}bpy)Ni^{II}(4-fluorophenyl)Br (**S14**) and paramagnetic Ni species (e.g., (t-^{Bu}bpy)Ni^{II}X$_2$ and [(t-^{Bu}bpy)Ni^{I}X]$_2$; see SI for analysis). Similar product mixtures have been observed in other stoichiometric oxidative studies with (bpy/phen)Ni^{I} complexes; Ni^{II} species are proposed to arise from rapid comproportionation of a putative Ni^{III} oxidative adduct with remaining Ni^{I}.[25,60]

Complexes **17** and **18** are also observed to activate the C(sp^2)–Cl bond of 1,4-chlorofluorobenzene (Figure 9). While the oxidative addition of aryl chlorides to (bpy/phen)Ni^{I} species has been invoked in methodologies,[65,66] it has not previously been demonstrated for a well-defined, isolable (bpy/phen)Ni^{I} complex.[25,37,63] Complex **18** is observed to convert the anticipated amount of aryl chloride within minutes, while **17** requires 24 hours of reaction time to reach the expected 50% conversion. This is perhaps due to the increased lability of olefinic stilbene relative to P(t-Bu)$_3$. Rigorous kinetic and mechanistic investigations into the reactivity profile of these complexes are beyond the scope of this study, but work is underway in our laboratory to further interrogate the behavior of this unique class of compounds.

CONCLUSIONS

In summary, we have identified a mild oxidative approach and precursor to a variety of Ni^{I} complexes bearing catalytically relevant ligands. These strategies enabled access to previously elusive complexes, including L$_1$Ni monophosphine dimers and the first examples of monomeric ^{t}-^{Bu}bpy-bound Ni^{I} species. For the monophosphine ligand class, we have elucidated structure–speciation relationships at Ni^{I} and their connection to ligand effects in Ni-catalyzed SMC reactions. For the bipyridine ligand class, we have synthesized and characterized well-defined monomeric complexes that are capable of activating aryl bromides and chlorides. We anticipate that our findings will enable future mechanistic studies and catalyst design for Ni-catalyzed cross-coupling reactions.

Supplementary Material

Refer to Web version on PubMed Central for supplementary material.

ACKNOWLEDGMENT

We thank Dr. Robert Taylor (UCLA) and Dr. Paul Oyala (Caltech) for assistance with EPR measurements and Dr. Saeed Khan (UCLA) for assistance with X-ray diffraction data collection. We thank Prof. Franziska Schoenebeck for helpful discussions. Financial support for this work was provided by the NIGMS (R35 GM126986). These studies were supported by shared instrumentation grants from the National Science Foundation under equipment grants CHE-1048804 and 2117480, along with the NIH Office of Research Infrastructure Programs under grant S10OD028644

REFERENCES

(1). Tasker SZ; Standley EA; Jamison TF Recent Advances in Homogeneous Nickel Catalysis. Nature 2014, 509, 299–309. [PubMed: 24828188]

(2). Ananikov VP Nickel: The “Spirited Horse” of Transition Metal Catalysis. ACS Catal. 2015, 5, 1964–1971.

(3). Su B; Cao Z-C; Shi Z-J Exploration of Earth-Abundant Transition Metals (Fe, Co, and Ni) as Catalysts in Unreactive Chemical Bond Activations. Acc. Chem. Res 2015, 48, 886–896. [PubMed: 25679917]

(4). Bajo S; Laidlaw G; Kennedy AR; Sproules S; Nelson DJ Oxidative Addition of Aryl Electrophiles to a Prototypical Nickel(0) Complex: Mechanism and Structure/Reactivity Relationships. Organometallics 2017, 36, 1662–1672.

(5). Diccianni JB; Diao T Mechanisms of Nickel-Catalyzed Cross-Coupling Reactions. Trends Chem. 2019, 1, 830–844.

(6). Chan AY; Perry IB; Bissonnette NB; Buksh BF; Edwards GA; Frye LI; Garry OL; Lavagnino MN; Li BX; Liang Y; Mao E; Millet A; Oakley JV; Reed NL; Sakai HA; Seath CP; MacMillan DWC Metallaphotoredox: The Merger of Photoredox and Transition Metal Catalysis. Chem. Rev 2022, 122, 1485–1542. [PubMed: 34793128]

(7). Malapit CA; Prater MB; Cabrera-Pardo JR; Li M; Pham TD; McFadden TP; Blank S; Minteer SD Advances on the Merger of Electrochemistry and Transition Metal Catalysis for Organic Synthesis. Chem. Rev 2022, 122, 3180–3218. [PubMed: 34797053]

(8). Richmond E; Moran J Recent Advances in Nickel Catalysis Enabled by Stoichiometric Metallic Reducing Agents. Synthesis 2017, 50, 499–513.

(9). Somerville RJ; Odena C; Obst MF; Hazari N; Hopmann KH; Martin R Ni(I)–Alkyl Complexes Bearing Phenanthroline Ligands: Experimental Evidence for CO_2 Insertion at Ni(I) Centers. J. Am. Chem. Soc 2020, 142, 10936–10941. [PubMed: 32520556]

(10). Somerville RJ; Martin R Relevance of Ni(I) in Catalytic Carboxylation Reactions. In Nickel Catalysis in Organic Synthesis: Methods and Reactions, Wiley, 2020; pp. 285–330.

(11). Charboneau DJ; Brudvig GW; Hazari N; Lant HMC; Saydjari AK Development of an Improved System for the Carboxylation of Aryl Halides through Mechanistic Studies. ACS Catal. 2019, 9, 3228–3241. [PubMed: 31007967]

(12). Tortajada A; Börjesson M; Martin R Nickel-Catalyzed Reductive Carboxylation and Amidation Reactions. Acc. Chem. Res 2021, 54, 3941–3952. [PubMed: 34586783]

(13). Beromi MM; Nova A; Balcells D; Brasacchio AM; Brudvig GW; Guard LM; Hazari N; Vinyard DJ Mechanistic Study of an Improved Ni Precatalyst for Suzuki–Miyaura Reactions of Aryl Sulfamates: Understanding the Role of Ni(I) Species. J. Am. Chem. Soc 2017, 139, 922–936. [PubMed: 28009513]

(14). Lin C-Y; Power PP Complexes of Ni(I): A “Rare” Oxidation State of Growing Importance. Chem. Soc. Rev 2017, 46, 5347–5399. [PubMed: 28675200]

(15). Bismuto A; Finkelstein P; Müller P; Morandi B The Journey of Ni(I) Chemistry. Helv. Chim. Acta 2021, 104, e202100177.

(16). Matsubara K; Fukahori Y; Inatomi T; Tazaki S; Yamada Y; Koga Y; Kanegawa S; Nakamura T Monomeric Three-Coordinate N-Heterocyclic Carbene Nickel(I) Complexes: Synthesis, Structures, and Catalytic Applications in Cross-Coupling Reactions. Organometallics 2016, 35, 3281–3287.

(17). Guven S; Kundu G; Weßels A; Ward JS; Rissanen K; Schoenebeck F Selective Synthesis of Z-Silyl Enol Ethers via Ni-Catalyzed Remote Functionalization of Ketones. J. Am. Chem. Soc 2021, 143, 8375–8380. [PubMed: 34033717]

(18). Beromi MM; Banerjee G; Brudvig GW; Charboneau DJ; Hazari N; Lant HMC; Mercado BQ Modifications to the Aryl Group of Dppf-Ligated Ni s-Aryl Precatalysts: Impact on Speciation and Catalytic Activity in Suzuki–Miyaura Coupling Reactions. Organometallics 2018, 37, 3943–3955. [PubMed: 31736532]

(19). Guard LM; Beromi MM; Brudvig GW; Hazari N; Vinyard DJ Comparison of Dppf-Supported Nickel Precatalysts for the Suzuki–Miyaura Reaction: The Observation and Activity of Nickel(I). Angew. Chem. Int. Ed 2015, 54, 13352–13356.

(20). Beromi MM; Banerjee G; Brudvig GW; Hazari N; Mercado BQ Nickel(I) Aryl Species: Synthesis, Properties, and Catalytic Activity. ACS Catal. 2018, 8, 2526–2533. [PubMed: 30250755]

(21). Kalvet I; Guo Q; Tizzard GJ; Schoenebeck F When Weaker Can Be Tougher: The Role of Oxidation State (I) in P- vs N-Ligand-Derived Ni-Catalyzed Trifluoromethylthiolation of Aryl Halides. ACS Catal. 2017, 7, 2126–2132. [PubMed: 28286695]

(22). Beromi MM; Brudvig GW; Hazari N; Lant HMC; Mercado BQ Synthesis and Reactivity of Paramagnetic Nickel Polypyridyl Complexes Relevant to C(sp^2)–C(sp^3)Coupling Reactions. Angew. Chem. Int. Ed 2019, 58, 6094–6098.

(23). Day CS; Rentería-Gómez Á; Ton SJ; Gogoi AR; Gutierrez O; Martin R Elucidating Electron-Transfer Events in Polypyridine Nickel Complexes for Reductive Coupling Reactions. Nat. Catal 2023, 6, 244–253.

(24). Standley EA; Smith SJ; Müller P; Jamison TF A Broadly Applicable Strategy for Entry into Homogeneous Nickel(0) Catalysts from Air-Stable Nickel(II) Complexes. Organometallics 2014, 33, 2012–2018. [PubMed: 24803717]

(25). Ting SI; Williams WL; Doyle AG Oxidative Addition of Aryl Halides to a Ni(I)-Bipyridine Complex. J. Am. Chem. Soc 2022, 144, 5575–5582. [PubMed: 35298885]

(26). Tsou TT; Kochi JK Mechanism of Oxidative Addition. Reaction of Nickel(0) Complexes with Aromatic Halides. J. Am. Chem. Soc 1979, 101, 6319–6332.

(27). Beck R; Shoshani M; Krasinkiewicz J; Hatnean JA; Johnson SA Synthesis and Chemistry of Bis(Triisopropylphosphine) Nickel(I) and Nickel(0) Precursors. Dalton Trans. 2012, 42, 1461–1475. [PubMed: 23169546]

(28). Newman-Stonebraker SH; Wang JY; Jeffrey PD; Doyle AG Structure–Reactivity Relationships of Buchwald-Type Phosphines in Nickel-Catalyzed Cross-Couplings. J. Am. Chem. Soc 2022, 144, 19635–19648. [PubMed: 36250758]

(29). Karl TM; Bouayad-Gervais S; Hueffel JA; Sperger T; Wellig S; Kaldas SJ; Dabranskaya U; Ward JS; Rissanen K; Tizzard GJ; Schoenebeck F Machine Learning-Guided Development of Trialkylphosphine Ni(I) Dimers and Applications in Site-Selective Catalysis. J. Am. Chem. Soc 2023, 145, 15414–15424. [PubMed: 37411044]

(30). Vilar R; Mingos DMP; Cardin CJ Synthesis and Structural Characterisation of [Pd2(μ-Br)2(PBut3)2], an Example of a Palladium(I)–Palladium(I) Dimer. J. Chem. Soc., Dalton Trans 1996, 4313–4314.

(31). Fricke C; Sperger T; Mendel M; Schoenebeck F Catalysis with Palladium(I) Dimers. Angew. Chem. Int. Ed 2021, 60, 3355–3366.

(32). Hueffel JA; Sperger T; Funes-Ardoiz I; Ward JS; Rissanen K; Schoenebeck F Accelerated Dinuclear Palladium Catalyst Identification through Unsupervised Machine Learning. Science 2021, 374, 1134–1140. [PubMed: 34822285]

(33). Zuo Z; Ahneman DT; Chu L; Terrett JA; Doyle AG; MacMillan DWC Merging Photoredox with Nickel Catalysis: Coupling of α-Carboxyl Sp^3-Carbons with Aryl Halides. Science 2014, 345, 437–440. [PubMed: 24903563]

(34). Huihui KMM; Caputo JA; Melchor Z; Olivares AM; Spiewak AM; Johnson KA; DiBenedetto TA; Kim S; Ackerman LKG; Weix DJ Decarboxylative Cross-Electrophile Coupling of N-Hydroxyphthalimide Esters with Aryl Iodides. J. Am. Chem. Soc 2016, 138, 5016–5019. [PubMed: 27029833]

(35). Zultanski SL; Fu GC Nickel-Catalyzed Carbon–Carbon Bond-Forming Reactions of Unactivated Tertiary Alkyl Halides: Suzuki Arylations. J. Am. Chem. Soc 2013, 135, 624–627. [PubMed: 23281960]

(36). Kawamata Y; Vantourout JC; Hickey DP; Bai P; Chen L; Hou Q; Qiao W; Barman K; Edwards MA; Garrido-Castro AF; deGruyter JN; Nakamura H; Knouse K; Qin C; Clay KJ; Bao D; Li C; Starr JT; Garcia-Irizarry C; Sach N; White HS; Neurock M; Minteer SD; Baran PS Electrochemically Driven, Ni-Catalyzed Aryl Amination: Scope, Mechanism, and Applications. J. Am. Chem. Soc 2019, 141, 6392–6402. [PubMed: 30905151]

(37). Sun R; Qin Y; Ruccolo S; Schnedermann C; Costentin C; Nocera DG Elucidation of a Redox-Mediated Reaction Cycle for Nickel-Catalyzed Cross Coupling. J. Am. Chem. Soc 2019, 141, 89–93. [PubMed: 30563318]

(38). Till NA; Oh S; MacMillan DWC; Bird MJ The Application of Pulse Radiolysis to the Study of Ni(I) Intermediates in Ni-Catalyzed Cross-Coupling Reactions. J. Am. Chem. Soc 2021, 143, 9332–9337. [PubMed: 34128676]

(39). Cagan DA; Bím D; McNicholas BJ; Kazmierczak NP; Oyala PH; Hadt RG Photogenerated Ni(I)–Bipyridine Halide Complexes: Structure–Function Relationships for Competitive C(sp^2)–Cl Oxidative Addition and Dimerization Reactivity Pathways. Inorg. Chem 2023, 62, 9538–9551. [PubMed: 37279403]

(40). Bismuto A; Müller P; Finkelstein P; Trapp N; Jeschke G; Morandi B One to Find Them All: A General Route to Ni(I)–Phenolate Species. J. Am. Chem. Soc 2021, 143, 10642–10648. [PubMed: 34251813]

(41). Ni S; Yan J; Tewari S; Reijerse EJ; Ritter T; Cornella J Nickel Meets Aryl Thianthrenium Salts: Ni(I)-Catalyzed Halogenation of Arenes. J. Am. Chem. Soc 2023, 145, 9988–9993. [PubMed: 37126771]

(42). Martinez GE; Ocampo C; Park YJ; Fout AR Accessing Pincer Bis(Carbene) Ni(IV) Complexes from Ni(II) via Halogen and Halogen Surrogates. J. Am. Chem. Soc 2016, 138, 4290–4293. [PubMed: 27014933]

(43). Zhou Y-Y; Hartline DR; Steiman TJ; Fanwick PE; Uyeda C Dinuclear Nickel Complexes in Five States of Oxidation Using a Redox-Active Ligand. Inorg. Chem 2014, 53, 11770–11777. [PubMed: 25337719]

(44). Evans DF 400. The Determination of the Paramagnetic Susceptibility of Substances in Solution by Nuclear Magnetic Resonance. J. Chem. Soc 1959, 2003–2005.

(45). Diccianni JB; Katigbak J; Hu C; Diao T Mechanistic Characterization of (Xantphos)Ni(I)-Mediated Alkyl Bromide Activation: Oxidative Addition, Electron Transfer, or Halogen-Atom Abstraction. J. Am. Chem. Soc 2019, 141, 1788–1796. [PubMed: 30612428]

(46). Ciszewski JT; Mikhaylov DY; Holin KV; Kadirov MK; Budnikova YH; Sinyashin O; Vicic DA Redox Trends in Terpyridine Nickel Complexes. Inorg. Chem 2011, 50, 8630–8635. [PubMed: 21797263]

(47). Dible BR; Sigman MS; Arif AM Oxygen-Induced Ligand Dehydrogenation of a Planar Bis-μ-Chloronickel(I) Dimer Featuring an NHC Ligand. Inorg. Chem 2005, 44, 3774–3776. [PubMed: 15907100]

(48). $[Ni(COD)Br]_2$ could also be synthesized using TMPhATB, but we found that use of TBATB as the oxidant led to less decomposition and higher yields.$_2$

(49). Porri L; Vitulli G; Gallazzi MC 1,5-Cyclooctadienenickel Bromide and Iodide. Angew. Chem. Int. Ed 1967, 6, 452.

(50). Lohrey TD; Cusumano AQ; Goddard WA; Stoltz BM Identifying the Imperative Role of Metal–Olefin Interactions in Catalytic C–O Reductive Elimination from Nickel(II). ACS Catal. 2021, 11, 10208–10222. [PubMed: 35186424]

(51). Newman-Stonebraker SH; Smith SR; Borowski JE; Peters E; Gensch T; Johnson HC; Sigman MS; Doyle AG Univariate Classification of Phosphine Ligation State and Reactivity in Cross-Coupling Catalysis. Science 2021, 374, 301–308. [PubMed: 34648340]

(52). Gensch T; Gomes G. dos P.; Friederich P; Peters E; Gaudin T; Pollice R; Jorner K; Nigam A; Lindner-D'Addario M; Sigman MS; Aspuru-Guzik A A Comprehensive Discovery Platform for

Organophosphorus Ligands for Catalysis. J. Am. Chem. Soc 2022, 144, 1205–1217. [PubMed: 35020383]

(53). Within minutes at ambient temperature in the solution phase, Ni^0 black and a color change from green to dark blue was observed for L_1Ni^I dimers with bulky phosphines (L = P(*t*-Bu)$_3$, CyP(*t*-Bu)$_2$). Per SCXRD analysis, the dark blue solution likely contains $Ni^{1.5+}$ dimer, as in $3.^0{}_1I_{32}{}^{1.5+}$

(54). For ligands smaller than P(*t*-Bu)$_3$ where more than one Ni^I species can form, L:Ni stoichiometry controlled the outcome for isolated material in the solid state. Speciation was generally conserved in solution-state NMR characterization (C_6D_6), though a small amount of phosphine dissociation and dimerization was observed for L_2Ni^I monomer 10 with CyP(*t*-Bu)$_{2\cdot3}{}^I{}_{662}{}^I{}_2$

(55). Cornella J; Gómez-Bengoa E; Martin R Combined Experimental and Theoretical Study on the Reductive Cleavage of Inert C–O Bonds with Silanes: Ruling out a Classical Ni(0)/Ni(II) Catalytic Couple and Evidence for Ni(I) Intermediates. J. Am. Chem. Soc 2013, 135, 1997–2009. [PubMed: 23316793]

(56). Brauer DJ; Krueger C Bonding of Aromatic Hydrocarbons to Nickel(0). Structure of Bis(Tricyclohexylphosphine)(1,2-η_2-Anthracene)Nickel(0)-Toluene. Inorg. Chem 1977, 16 (4), 884–891.

(57). Hoberg H; Radine K; Krüger C; Romão MJ Synthesis of New Phosphine Nickel(I) Complexes and Crystal Structure of μ3-Iodo-Tris-μ-Iodo-Cyclotris(Triphenylphosphine Nickel), $(TPP)_3Ni_3I_4$. Z. Naturforsch. B 1985, 40, 607–614.

(58). Borowski JE; Newman-Stonebraker SH; Doyle AG Comparison of Monophosphine and Bisphosphine Precatalysts for Ni-Catalyzed Suzuki–Miyaura Cross-Coupling: Understanding the Role of the Ligation State in Catalysis. ACS Catal. 2023, 13, 7966–7977.

(59). Sheng J; Ni H-Q; Liu G; Li Y; Wang X-S Combinatorial Nickel-Catalyzed Monofluoroalkylation of Aryl Boronic Acids with Unactivated Fluoroalkyl Iodides. Org. Lett 2017, 19, 4480–4483. [PubMed: 28809568]

(60). Hamby TB; LaLama MJ; Sevov CS Controlling Ni Redox States by Dynamic Ligand Exchange for Electroreductive Csp^3–Csp^2 Coupling. Science 2022, 376, 410–416. [PubMed: 35446658]

(61). Nattmann L; Saeb R; Nöthling N; Cornella J An Air-Stable Binary Ni(0)–Olefin Catalyst. Nat. Catal 2020, 3, 6–13.

(62). Wilke G; Mueller EW; Kroener M; Heimbach P; Breil H CO- and NO- Free Complexes of Transition Metals. DE-1191375, April 22, 1965.

(63). Lin Q; Diao T Mechanism of Ni-Catalyzed Reductive 1,2-Dicarbofunctionalization of Alkenes. J. Am. Chem. Soc 2019, 141, 17937–17948. [PubMed: 31589820]

(64). Humphrey ELBJ; Kennedy AR; Sproules S; Nelson DJ Evaluating a Dispersion of Sodium in Sodium Chloride for the Synthesis of Low-Valent Nickel Complexes. Eur. J. Inorg. Chem 2022, e202101006.

(65). Mirabi B; Marchese AD; Lautens M Nickel-Catalyzed Reductive Cross-Coupling of Heteroaryl Chlorides and Aryl Chlorides. ACS Catal. 2021, 11, 12785–12793.

(66). Yue H; Zhu C; Rueping M Cross-Coupling of Sodium Sulfinates with Aryl, Heteroaryl, and Vinyl Halides by Nickel/Photoredox Dual Catalysis. Angew. Chem. Int. Ed 2018, 57, 1371–1375.

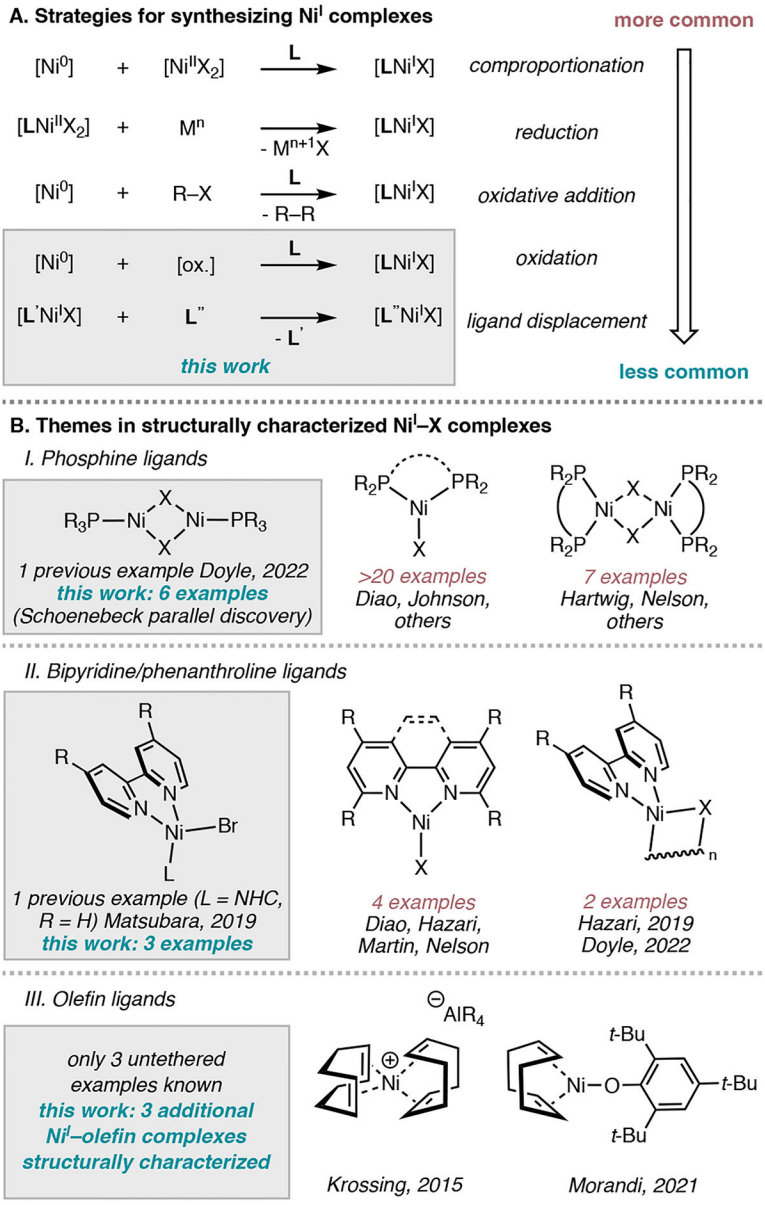

Figure 1.

(A) Ni^{I} complex synthetic strategies and their prevalence. (B) Examples of structurally characterized Ni^{I} complexes for (I) phosphine ligands, (II) bipyridine/phenanthroline ligands, and (III) olefin ligands with no other coordinating atom.

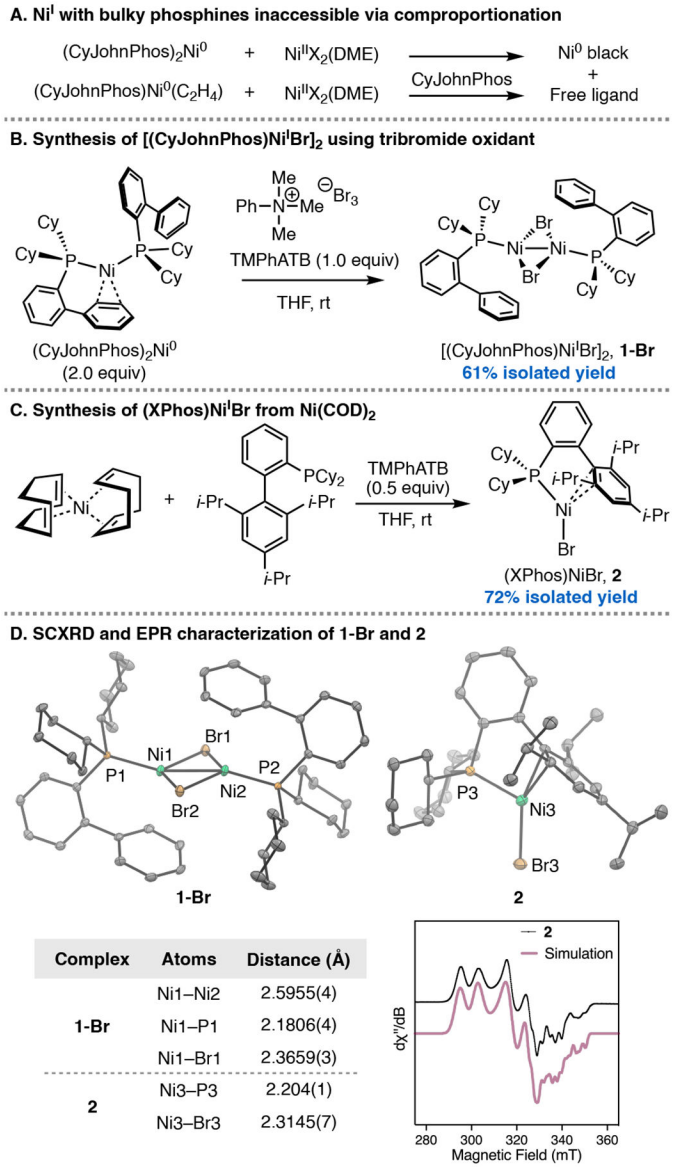

Complex	Atoms	Distance (Å)
1-Br	Ni1–Ni2	2.5955(4)
	Ni1–P1	2.1806(4)
	Ni1–Br1	2.3659(3)
2	Ni3–P3	2.204(1)
	Ni3–Br3	2.3145(7)

Figure 2.

(A) Attempted syntheses of **1-Cl** and **1-Br** via comproportionation (X = Cl or Br). (B) Initial discovery of tribromide oxidation to generate **1-Br**. (C) One-pot oxidation from $Ni(COD)_2$ to give **2**. (D) Solid state structures of **1-Br** and **2**, with thermal ellipsoids displayed at 50% probability and hydrogen atoms omitted for clarity. Selected solid-state bond distances are tabulated. EPR simulation parameters: g_1 = 2.306, g_2 = 2.138, g_3 = 2.039. For simulated hyperfine splitting and strain, see SI.

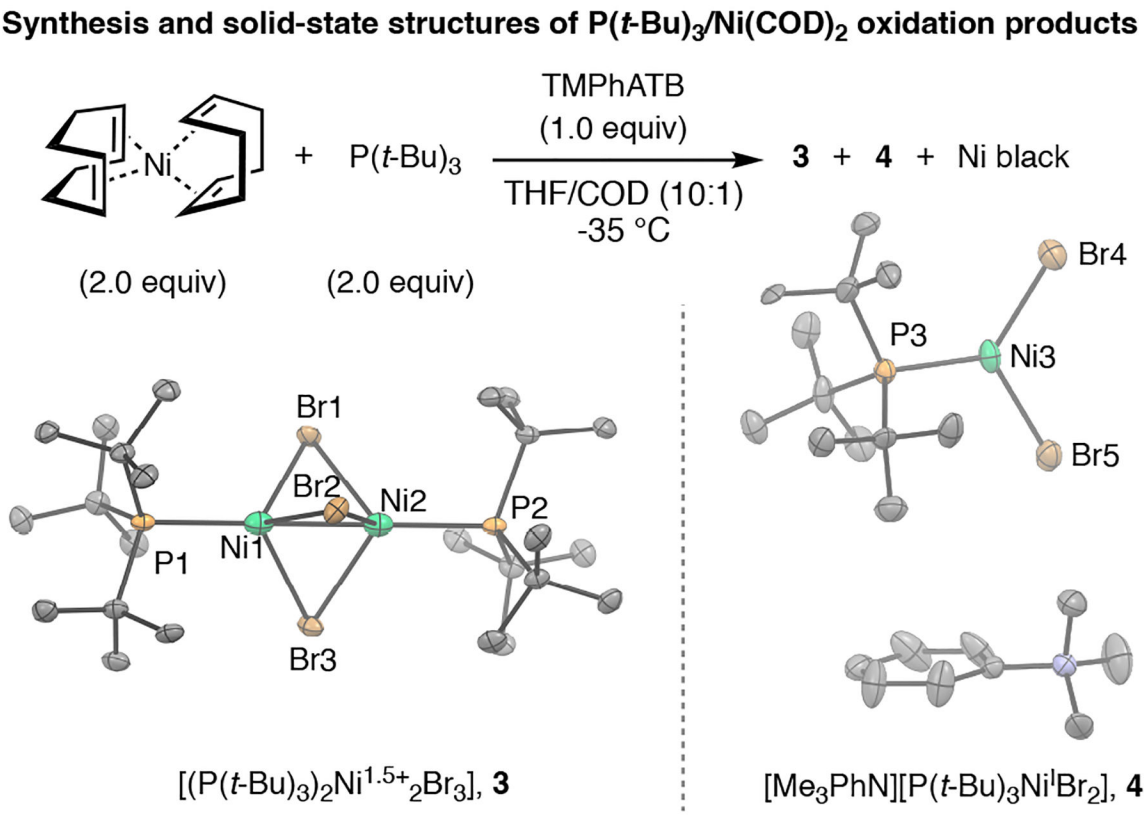

Figure 3.

Synthesis and solid state structures of **3** and **4**, with thermal ellipsoids displayed at 50% probability and hydrogen atoms omitted for clarity. Selected bond distances (Å) for **3**: Ni1–Ni2: 2.378(1); Ni1–P1: 2.306(1); Ni1–Br1: 2.4637(1). Selected bond distances (Å) for **4**: Ni3–P3: 2.209(1); Ni3–Br4: 2.4096(7).

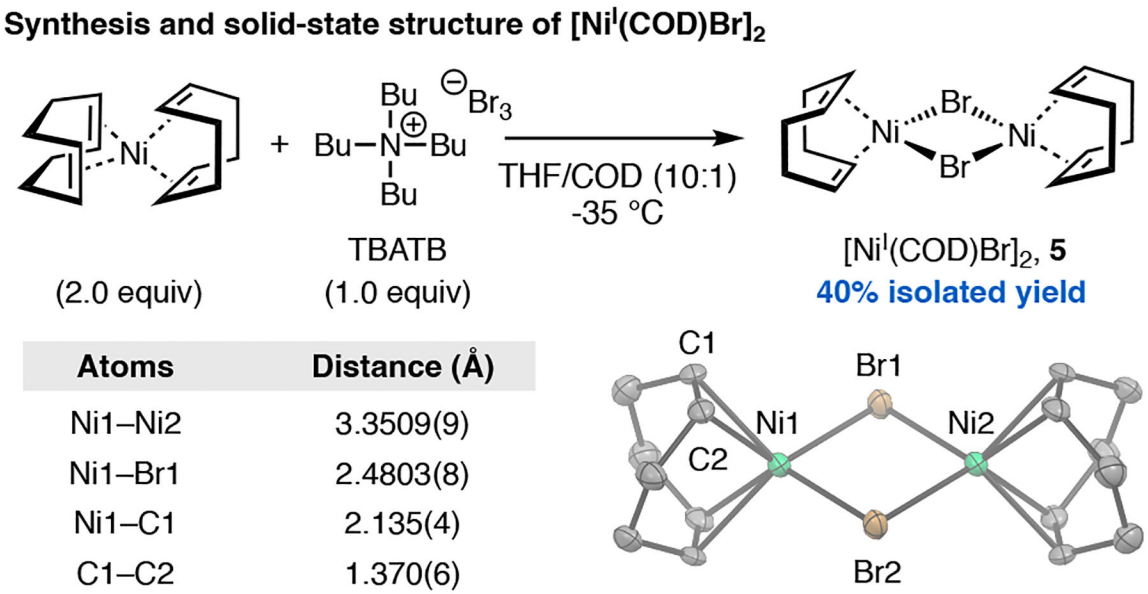

Atoms	Distance (Å)
Ni1–Ni2	3.3509(9)
Ni1–Br1	2.4803(8)
Ni1–C1	2.135(4)
C1–C2	1.370(6)

Figure 4.

Synthesis, selected interatomic distances, and solid state structure of **5**. Thermal ellipsoids are displayed at 50% probability and hydrogen atoms are omitted for clarity. Selected solid-state bond distances are tabulated.

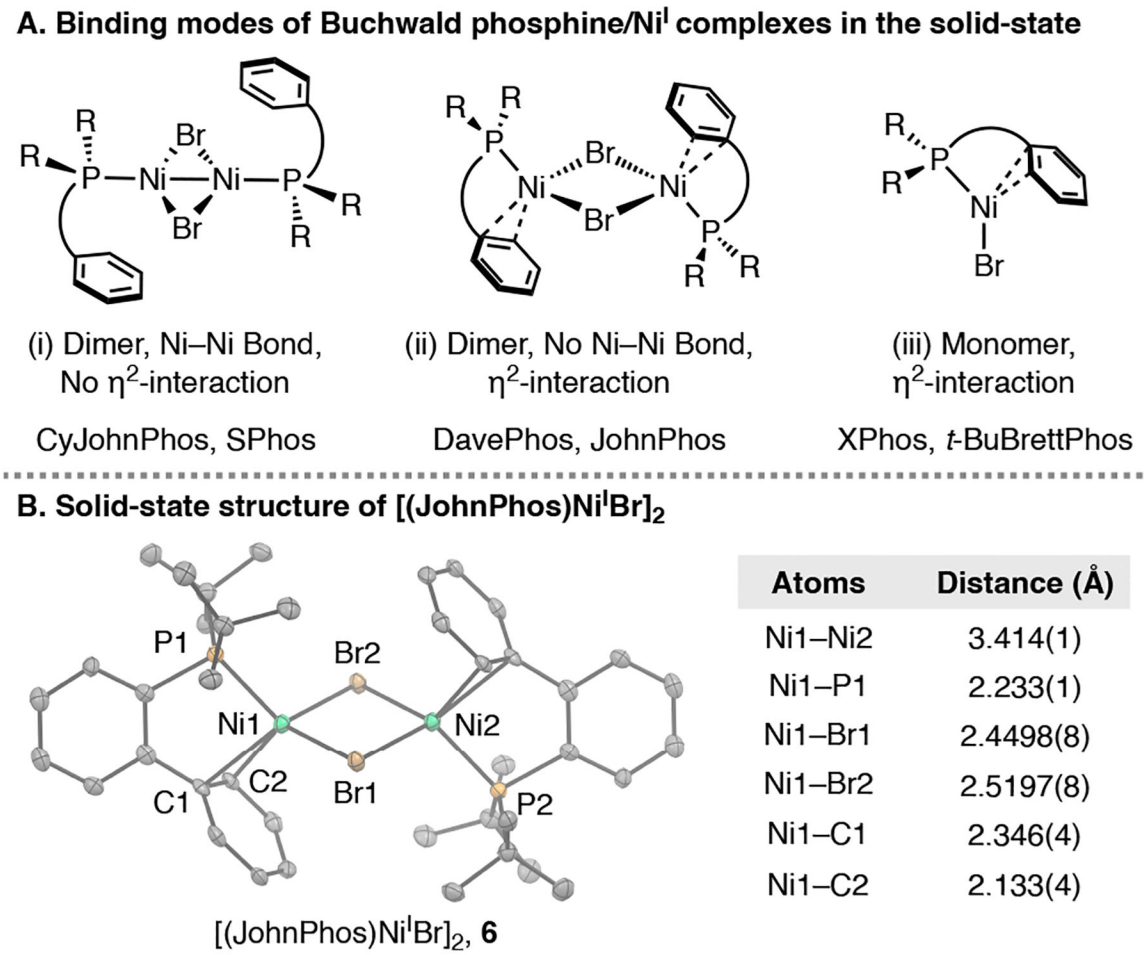

Atoms	Distance (Å)
Ni1–Ni2	3.414(1)
Ni1–P1	2.233(1)
Ni1–Br1	2.4498(8)
Ni1–Br2	2.5197(8)
Ni1–C1	2.346(4)
Ni1–C2	2.133(4)

Figure 5.

(A) Buchwald ligand-bound Ni^{I} complex binding modes in the solid state. (B) Solid-state structure of $[(JohnPhos)Ni^{I}Br]_2$ (**6**) with thermal ellipsoids displayed at 50% probability and hydrogen atoms omitted for clarity.

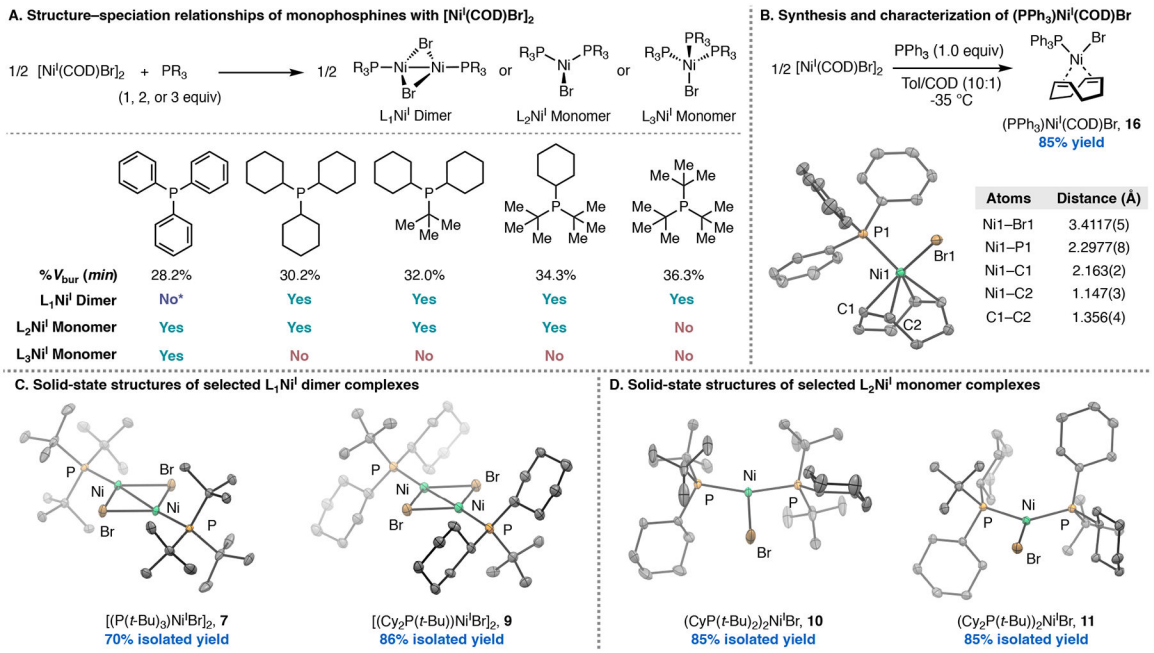

Figure 6.

(A) Monophosphine structure–speciation relationships. (B) Synthesis and structural characterization of $(PPh_3)Ni^I(COD)Br$. (C) Solid-state structures of selected L_1Ni^I dimers, with thermal ellipsoids displayed at 50% probability and hydrogen atoms omitted for clarity. (D) Solid-state structures of selected L_2Ni^I monomers, with thermal ellipsoids displayed at 50% probability and hydrogen atoms omitted for clarity.

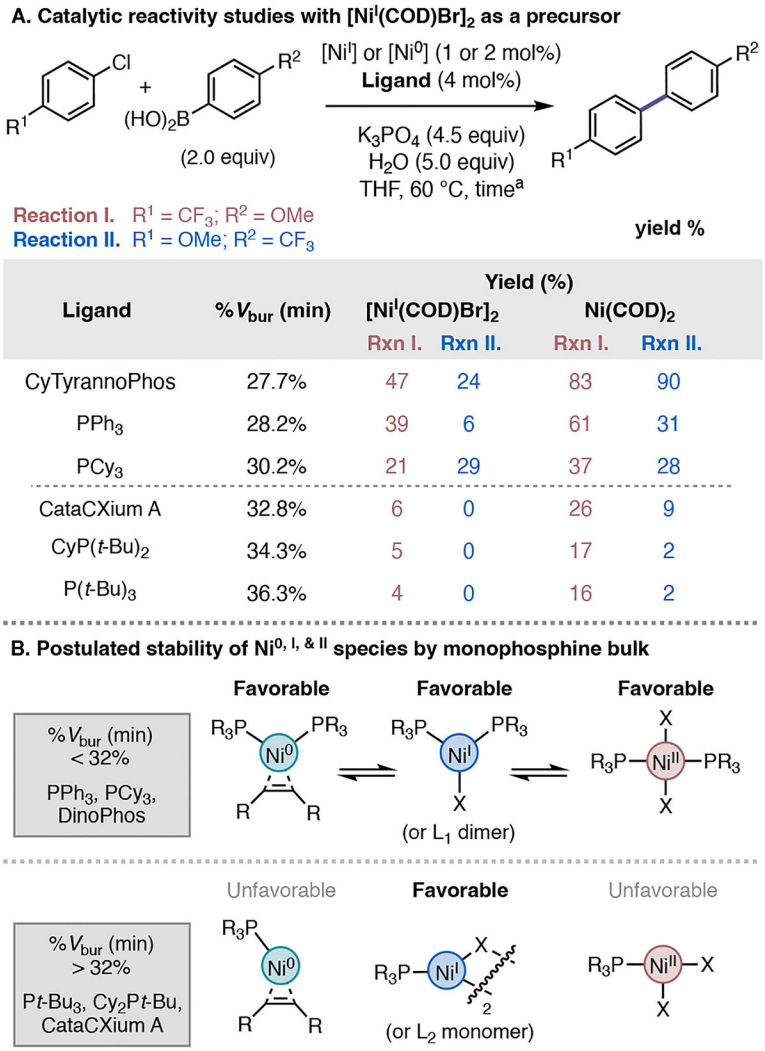

Ligand	% V_{bur} (min)	Yield (%) [Ni^I(COD)Br]2 Rxn I.	Yield (%) [Ni^I(COD)Br]2 Rxn II.	Yield (%) Ni(COD)2 Rxn I.	Yield (%) Ni(COD)2 Rxn II.
CyTyrannoPhos	27.7%	47	24	83	90
PPh_3	28.2%	39	6	61	31
PCy_3	30.2%	21	29	37	28
CataCXium A	32.8%	6	0	26	9
$CyP(t\text{-}Bu)_2$	34.3%	5	0	17	2
$P(t\text{-}Bu)_3$	36.3%	4	0	16	2

Figure 7.

(A) Catalytic reactivity studies comparing **5** and $Ni(COD)_2$ as precatalysts in an SMC reaction. [a]Rxn. I run for 45 min. and Rxn. II run for 2 hours. (B) Rationalization of catalytic reactivity by thermodynamic favorability of phosphine steric environment across oxidation states.

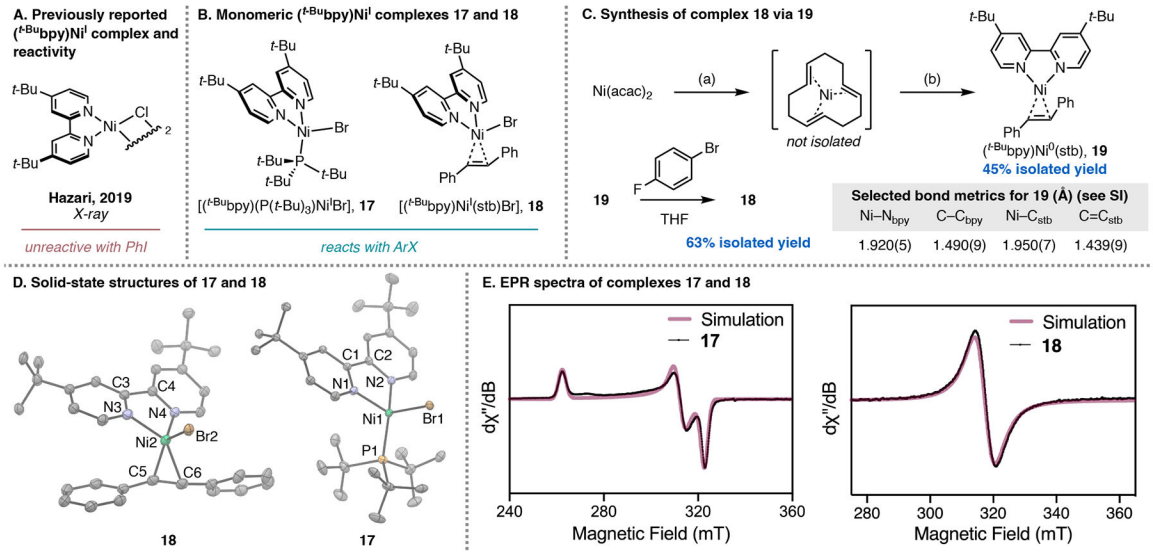

Figure 8.

(A) Precedented dimeric (*t*-Bubpy)Ni^{I} halide complex and reactivity. (B) Monomeric (*t*-Bubpy)(L)Ni^{I}Br complexes accessed in this work. (C) Synthesis of complex **18** via complex **19**. Conditions (a): 1.35 equiv (*E, E, E*)-1,5,9-cyclododecatriene, 2.3 equiv Al(OEt)Et_2, Et_2O, −35 °C to rt, 16 h. Conditions (b): 1 equiv stb, 1 equiv *t*-Bubpy, Et_2O. (D) Solid-state structures of **17** and **18**, with thermal ellipsoids displayed at 30% probability and hydrogen atoms omitted for clarity. Selected solid-state bond distances (Å) for **17**: Ni1–P1: 2.249(1); Ni1–Br1: 2.4438(7); Ni1–N1: 1.983(3); N1–C1: 1.365(3); C1–C2: 1.472(3). Selected solid-state bond distances (Å) for **18**: Ni2–Br2: 2.4062(6); Ni2–N3: 1.997(3) N3–C3: 1.351(4); C3–C4: 1.471(4); Ni2–C5: 2.057(5); C5–C6: 1.406(5). (E) X-band EPR spectra of **17** (toluene glass, 77 K) and **18** (THF, 298 K). Simulation parameters (**17**): g_1 = 2.557, g_2 = 2.148, g_3 = 2.077. Simulation parameters (**18**): g_{iso} = 2.211. Synthesis of **17** from **7** not shown. See SI for more information.

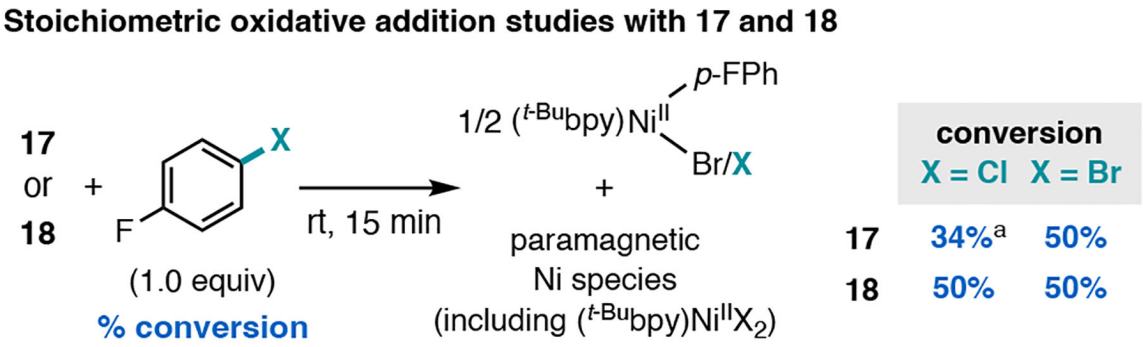

Figure 9.

Stoichiometric reactivity with aryl halides for **17** and **18**. [a]Conversion measured after 4 h.

Table 1.

Ligand generality of tribromide oxidation

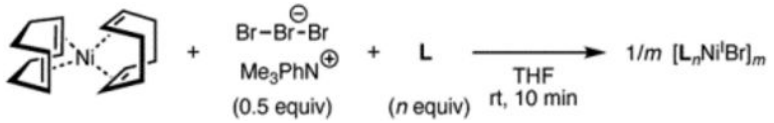

Ligand	*n*	Ni^{I} complex	Br_3^- oxidation yield (isolated)
PPh_3	3	$\mathbf{L}_3Ni^{I}Br$	**75%**
PCy_3	2	$\mathbf{L}_2Ni^{I}Br$	**67%**
dppf	1	$\mathbf{L}Ni^{I}Br/[\mathbf{L}Ni^{I}Br]_2$	**77%**
t-BuXantPhos	1	$\mathbf{L}Ni^{I}Br$	**48%**
IPr	1	$[\mathbf{L}Ni^{I}Br]_2$	**69%**
tpy	1	$\mathbf{L}Ni^{I}Br$	**42%**
$^{t\text{-}Bu}$bpy	1	$[\mathbf{L}Ni^{I}Br]_2$	**66%** [a]

[a]NMR yield using displaced COD as an internal standard